Proceedings of the Combustion Institute 34 (2013) 1949–1956
Y. Nagura, J. Kasahara, Y. Sugiyama, A. Matsuo

Title: **Comprehensive Visualization of Detonation-Diffraction Structures and Sizes in Unstable and Stable Mixtures**

Authors: YUUTO NAGURA[1], JIRO KASAHARA[1], YUTA SUGIYAMA[2] AND AKIKO MATSUO[2]

Affiliation 1: Department of Engineering Mechanics and Energy, University of Tsukuba, Tennodai 1-1-1, Tsukuba 305-8573, Japan.

Affiliation 2: Department of Mechanical Engineering, Keio University, Hiyoshi 3-14-1, Kohoku-ku, Yokohama 223-8522, Japan.

Address: Department of Engineering Mechanics and Energy, Jiro Kasahara, University of Tsukuba, Tennodai 1-1-1, Tsukuba 305-8573, Japan.

Fax: +89-29-853-5267

E-mail: kasahara@kz.tsukuba.ac.jp

Colloquium: Detonations, Explosions and Supersonic Combustion

Total length: 6200 words (Method M1)

Main text: 2963 words

Nomenclature: 114 words

References: 315 words

Tables: 259 words

Figures: 2549 words

Proceedings of the Combustion Institute 34 (2013) 1949–1956
Y. Nagura, J. Kasahara, Y. Sugiyama, A. Matsuo

Abstract

The geometry and characteristic length of diffraction and re-initiation during two-dimensional detonation propagation were revealed by visualization. $C_2H_4+3O_2$ (unstable), $2C_2H_2+5O_2+7Ar$ (stable) and $2C_2H_2+5O_2+21Ar$ (stable) were used as the test mixture**s**. Experiments were performed over the deviation angle range from 30° to 150° and the initial pressure range from 15.8 kPa to 102.3 kPa. By self-emitting photography, we confirmed that the geometry and the characteristic length of diffraction are not different among test gasses, with the exception of the fan-like structure of re-initiation that occurred regardless of whether the mixture was unstable or stable. We conducted a compensative experiment by changing the deviation angle and initial pressure, and summarized the detonation diffraction by shadowgraph. At deviation angles larger than 60°, we measured the distances from the vertex of the channel corner to the point where the transverse detonation wave reflected on the under wall (= wall reflection distance) and confirmed that wall reflection distances are approximately in the range of 10-15 times the cell width, whether the mixture is unstable or stable.

Nomenclature

Ea	=	Arrhenius activation energy
L_c	=	dimensionless characteristic length of diffraction
p_0	=	initial pressure of the mixture
r_w	=	the wall reflection distance

R	=	gas constant
T	=	temperature of the mixture
t	=	time after detonation wave diffraction
t_e	=	exposure time of the high-speed video camera
W	=	depth of the channel plate
λ	=	cell width
θ_d	=	angle of the channel plate

Keywords

detonation initiation, detonation diffraction, visualization, activation energy

1 Introduction

When a planar detonation wave emerges from a tube into unconfined space filled with a gaseous mixture, detonation wave diffraction may occur due to the abrupt change in the cross-section area. The shape of the detonation wave change from a plane to a curve, and the expansion waves generated from the vertex of the tube exit attenuate the detonation wave. As a result, the shock wave constituting the detonation wave is decoupled from the reaction front [1-4]. If the shock wave front is completely decoupled from the reaction front, the detonation wave is quenched (subcritical case). However, if the tube diameter is larger than the critical tube diameter, the detonation wave may re-initiate and propagate into unconfined space (supercritical case).

Detonation wave diffraction is affected by the deviation angle of the flow channel [5-7]. Khasainov et al. [8] investigated the effect of the deviation angle on the re-initiation process with soot foil by changing the angle of the flow channel like a fan from 5° to 90°. When the deviation angle was smaller than 40°, the re-initiation point originated in the vicinity of the channel wall, but when the deviation angle was larger than 40°, the local re-initiation point originated at the tube axis. Nagura et al. [9] visualized the re- initiation of detonation in a C_2H_4+3O_2 mixture with a high-speed video camera while changing the deviation angle from 30° to 150°. They suggest that the transverse detonation wave may originate at 11.1 times the cell width from the vertex of the channel corner and be reflected on the lower channel wall at 12.3 times the cell width from the vertex.

Arienti and Shepherd [10] conducted a detailed numerical analysis to investigate the effect of activation energy on detonation diffraction, presupposing a single-step reaction in the Arrhenius form. They revealed that the behavior of diffraction is affected by activation energy. Pintgen and Shepherd [11] investigated the effect of activation energy

on critical (boundary between subcritical and supercritical) diffraction and subcritical diffraction, and remarked that the detonation diffraction is not affected by thermodynamic properties but is linked to the larger activation energy.

Lee [12] suggested that detonation diffraction exhibits two types of propagating structure, unstable and stable. Re-initiation in an unstable mixture that has high activation energy such as non-diluted C_2H_2-O_2 is affected by a transverse wave predominately, and it begins with a detonation bubble originating from the tube axis. On the other hand, in a stable mixture that has low activation energy such as Ar-diluted C_2H_2-O_2, a transverse detonation wave is secondary for re-initiation, while the effect of the wave curvature is dominant.

To date there has been no study that investigated under varied experimental conditions whether the dominant factor of the detonation diffraction structure is the curvature (cell width or induction length as the characteristic length) or the activation energy. Thus, in the present study, we conducted an experiment using three kinds of test mixture (C_2H_4+3O_2, 2C_2H_2+5O_2+7Ar and 2C_2H_2+5O_2+21Ar) and investigated the effect of the mixture stability (unstable or stable), the initial pressure and the deviation angle on the position of re-initiation, the geometry and the size of the shock front in diffraction compensatively. However, in the present study, to determine the fundamental diffraction structure, we focused on only the supercritical case, which allowed us to ignore the effect of the tube diameter.

2 Experimental apparatus

The observation chamber and optical system were set up so that we could observe the detonation propagation and diffraction in a rectangular cross-section tube. Figure 1 shows the side view of the observation chamber and the visualization region. The observation chamber consists of rectangular tubes, 20 mm wide by 16 mm deep, and square channel plates, 100 mm on a side. A detonation tube was put in the bottom of the observation chamber, and a dump tank was put in the left top part of the chamber. A planar detonation wave originating in the detonation tube emerged in the observation chamber, and then after the detonation wave passed through the channel plate, a high-pressure, high-temperature gas was discharged into the dump tank. At this time, the detonation diffraction and re-initiation in the observation region were observed by using a high-speed video camera. The observation region can be changed to a given shape by using channel plates. It has four choices of deviation angle (θ_d = 30°, 60°, 90° and 150°) and two choices of thickness (2 mm and 16 mm).

Three kinds of mixture were used so that we could consider activation energy, i.e., the stability or instability of the cell structure under the experimental conditions. We used C2H4+3O2 as the unstable mixture, and $2C_2H_2+5O_2+7Ar$ and $2C_2H_2+5O_2+21Ar$ as the stable mixtures. The range of initial pressure of the filling mixture was from 20 kPa to 100 kPa at room temperature. Under those conditions, the detonation wave was re-initiated in all mixtures under a supercritical diffraction condition.

Shadowgraph and multi-frame-short-time open-shutter photography (MSOP) [13] were used as the optical system. MSOP can observe the shape of a wave and the cell structure at the same time by observing the self-emitting luminosity of the detonation during a respectively-long exposure time. The frame interval was from 1 μs to 4 μs,

and the exposure time was 1/4 of the frame interval. The spatial resolution of the images was approximately 0.3 mm.

3 Results and discussion

3.1 Comparison of unstable and stable mixtures by MSOP

To observe what kind of effects unstable or stable cell structure has on two-dimensional detonation diffraction, we conducted visualization by MSOP using the channel plate of $\theta_d = 90°$ and 2 mm in depth. Table 1 summarizes the experimental conditions. Figure 2 shows the MSOP images of detonation diffraction arranged at a fixed time interval. The upper images are under unstable conditions, and the lower images are under stable conditions. The initial pressures are much higher than the propagation limit under both sets of conditions, so they are considered to be supercritical conditions. The frame speed was different for each image, so we defined a dimensionless characteristic length $L_C = \frac{V_{CJ} \times t}{\lambda}$ using Chapman-Jouguet (CJ) velocity V_{CJ}, time after detonation diffraction t and cell width λ. (the CJ velocity was computed using CEA of NASA, and the cell width was referred from the Caltech detonation database) to make the time scale the same for all images. White solid lines in Fig. 2 show the shapes of the flow channel**.** Moreover, Fig. 3 shows the model image of two-dimensional detonation diffraction.

In terms of the unstable mixture, Fig. 2a shows that the detonation wave is curved in the vicinity of the corner, due to expansion waves, and the shock front is decoupling from the reaction front. However, the attenuation effect of two-dimensional expansion waves is milder than that of three-dimensional waves, so the cell structures seem to remain at the head of the expansion wave (corresponding to Fig. 3b). Interestingly, in Fig. 2b, a fan-like structure (point R) can be observed in the upper left of the corner. This structure may be the re-initiation point of detonation.

A fine cell structure can be observed on the right side of point R, while on the left side it cannot, so point R may originate at the boundary of existence and non-existence of cell structures (corresponding to Fig. 3 c). In Fig. 2c, there is a strong light-emitting line on the wave front. This luminosity is attributable to a strong exothermal reaction caused by a transverse detonation wave propagating in the shock-induced but unburned mixture (corresponding to Fig. 3e). A schlieren photograph of this phenomenon was shown by Pintgen and Shepherd [10]. In Fig. 2d, the transverse detonation wave approaches the lower channel wall, and the diffracted detonation wave is completely recovered. In the present study, this point is called the wall reflection point, and we defined wall reflection distance r_w as the distance from the vertex of the channel corner to the wall reflection point (corresponding to Fig. 3g).

We also examined the stable condition. Figure 2e shows that the detonation wave is curved in the vicinity of the corner due to expansion waves, just like in the unstable condition. The cell structure seems to be maintained on the upper side of the corner despite the expansion waves. Figure 2f shows that the detonation front recovers by re-initiation, and there are very regular cell structures. During the exposure time of this experiment, the fan-like structure of re-initiation, like that in the unstable condition, can be observed. However, there is a strong self-emitting luminosity by a transverse detonation wave of re-initiation at the extreme left side of the wave front. In Fig. 2g, the detonation wave has completely recovered.

In conclusion, the stable condition is very similar to the unstable condition, with the exception that the re-initiation point (point R) consisting of a complex triple-point structure cannot be observed in the stable condition. Since both wave fronts abruptly recovered by the transverse detonation wave propagating in the shocked but unburned mixture, the transverse wave originating on the upper side of the corner plays an important role in

two-dimensional detonation re-initiation, despite the stability of the cell structure. In other words, in a two-dimensional flow, the effect of activation energy is secondary as a cause of re-initiation. The dominant factor is a hot spot produced by the interaction between the strength of a transverse wave from a non-decoupled detonation wave and the curvature.

3.2 Effect of the initial pressure and the deviation angle on the diffraction

In the present section, we change the initial pressure of the mixture and the deviation angle of the channel plate in addition to the kind of mixture, and investigate the effect on the diffracting features, in particular on the wall reflection point.

Table 2 shows all of the experimental conditions. Four kinds of channel plate (θ_d = 30°, 60°, 90° and 150°) were used in these experiments. Here, we used a 16-mm-deep channel plate instead of a 2-mm-deep channel plate. We used three kinds of test mixture, C_2H_4+3O_2, 2C_2H_2+5O_2+7Ar and 2C_2H_2+5O_2+21Ar, and the range of initial pressure was from 15.8 kPa to 102.3 kPa (in regard to each mixture, the detonation wave was quenched at less than the minimum initial pressure shown in Table 2). The framing speed of the high-speed video camera was 1 μs/frame, and the exposure time was 250 ns.

The pictures shown in Fig. 4 and Fig. 5 were composed by superimposing the detonation fronts and the shock fronts at 2-μs intervals and 3-μs intervals, respectively. The gradations were inverted in both figures.

Figure 4 shows the detonation diffraction in the C_2H_4+3O_2 mixture (unstable). The pictures in the upper row are arranged in the following order: θ_d = 30°, 60°, 90° and 150°, and in the following order of the left column: p_0 = 20

kPa, 50 kPa and 100 kPa. Figure 4 shows that the interspaces and the time scale of detonation diffraction become small with increasing p_0. This is why the cell width becomes small with increasing p_0. Despite the differences in diffraction scale associated with the initial pressure, the origin of re-initiation and the shapes of the diffracting wave front seem to be similar. When we focus on the deviation angle, we can see that the region where the shock front is decoupled from the reaction front becomes large with increasing deviation angle. The transverse detonation wave that originated with re-initiation (in Fig. 4, we can see it as the black point at the extreme left of the wave front) propagates along the decoupled shock wave, so the trajectory of the transverse wave will be affected by flow channel geometry. On the other hand, Nagura et al. showed that the transverse detonation wave originates at 11.1 times the cell width from the corner regardless of the deviation angle. In other words, the deviation angle affects the shapes of detonation diffraction after re-initiation, but it does not affect the structures before re-initiation.

Figure 5 shows the detonation diffraction in the $2C_2H_2+5O_2+21Ar$ mixture (stable). The pictures are arranged in the following order in the left column: p_0 = 20 kPa, 50 kPa and 100 kPa. Comparing Fig. 4 with Fig. 5, we can see that the scales of diffraction in the $2C_2H_2+5O_2+21Ar$ mixture (stable) are larger than in the $C_2H_4+3O_2$ mixture (unstable). This is why the cell width and CJ velocity differ based on the mixture, but there is less difference between the unstable and stable mixtures with regard to the shape of the diffracting wave front, so the re-initiation structure may be the same whether the mixture is unstable or stable.

To compare the scale of detonation diffraction in an unstable and a stable mixture quantitatively, we measured the wall reflection distance, r_w, shown in Fig. 2 as the characteristic length in $C_2H_4+3O_2$, $2C_2H_2+5O_2+7Ar$ and $2C_2H_2+5O_2+21Ar$. We defined r_w as the distances from the vertex of the corner to the point where a transverse

detonation wave contacts the bottom wall. The systematic error derived from camera resolution was within ±1 pixel = ±0.3 mm.

Figures 6 and 7 show graphs plotting dimensionless wall reflection distance r_w/λ to p_0 according to θ_d in $C_2H_4+3O_2$ and both $2C_2H_2+5O_2+7Ar$ and $2C_2H_2+5O_2+21Ar$, respectively. The values of cell width obtained for the same kind of mixture as that used in the present study were extracted from the Caltech detonation database [14]. However, the value in Fig. 6 is the average of the data from three experiments, and the value in Fig. 7 is the data from a single experiment. In the case of $\theta_d = 30°$, the detonation wave is decoupled only a little, so we were unable to measure r_w.

Figure 6 shows that the dimensionless wall reflection distance, r_w/λ, is 8.2 - 15.5. At $p_0 \leq 30$ kPa, r_w/λ tends to vary, due to approaching limit of propagation; however, at 60 kPa $\leq p_0$ r_w/λ became constant at θ_d. Since the velocity of the shock wave after diffracting decreases with increasing θ_d, the distance from the vertex of the corner to the point where the transverse detonation wave propagating along the shock front reflects on the lower channel wall (i.e., r_w) becomes short. Figure 7 shows that the dimensionless wall reflection point r_w/λ becomes constant despite p_0. In this case, r_w/λ is 8.2 - 11.5 for $2C_2H_2+5O_2+7Ar$ and 13.7 - 17.9 for $2C_2H_2+5O_2+21Ar$. In other words, if we focus on a given deviation angle, the wall reflection point r_w is approximately 10 - 15 times the cell width regardless of whether the mixture was unstable or stable.

Finally, in order to understand the mechanism of re-initiation, numerical simulations were conducted. The governing equations are the compressible and reactive two-dimensional Euler equations, which are integrated by a third-order total variation diminishing Runge–Kutta scheme [15]. The fluid is an ideal gas with constant specific

heat ratio of 1.4. A two-step—which denotes induction and exothermic steps—reaction model by Korobeinikov et al. [16] is used to model the chemical reactions. The parameters in the present simulation are the same as those of Korobeinikov et al. [16], and premixed gas is modeled as stoichiometric H_2-air. The numerical simulation with complex mixture such as C_2H_2-O_2-Ar is very difficult, so we used a less complex mixture – H_2-air (stable). Initial pressure and temperature are 1.0 atm, and 293 K, respectively.

Figure 8 shows triple point trajectory (a) and temperature (b). In Fig. 8a, there is a fan-like structure on the upper left of the corner. This structure may be the same phenomenon as the point R in Fig. 2b and re-initiation occurs at this fan center. Figure 8b shows that the transverse detonation wave propagates from the front edge of the fan to the lower wall. After this, the transverse detonation is expected to reflect on the lower wall at a distance of about 20 times the cell width from the channel corner. This value is larger than the experimental result that the wall reflection distance r_w is within 10 - 15 times the cell width. This is suspected to be caused by the difference between two-dimensional simulations and three-dimensional experiments. The experimental result was slightly affected by the depth of the channel, but the numerical simulation was completely two-dimensional, so instability might be reduced. However, the wave shape of simulation is quite similar to the experimental result, so it is suggested that the mechanism of detonation diffraction tends to be the same in any mixture, and it is defined roughly by cell width.

Conclusions

The two-dimensional detonation diffraction was visualized in unstable and stable mixtures with a high-speed video camera. We used multi-frame-short-time open-shutter photography and observed both the cell structure and the wave geometry in $C_2H_4+3O_2$ (unstable) and $2C_2H_2+5O_2+21Ar$ (stable) mixtures. In the unstable mixture, re-initiation originated on the upper side of the vertex of the channel corner and cell structures recovered by a transverse detonation wave. In the stable mixture, we couldn't observe the fan-like structure of re-initiation shown in the unstable mixture. However, the diffraction structure in the stable mixture was very similar to that in the unstable mixture, so they showed no significant difference.

We also measured the positions of the wall reflection point and investigated the dependency on the deviation angle, θ_d, and initial pressure, p_0, and summarized the comprehensive visualization pictures. Three kind of mixtures, $C_2H_4+3O_2$, $2C_2H_2+5O_2+7Ar$ and $2C_2H_2+5O_2+21Ar$, were used. We confirmed that diffracting interspace and time were decreased with increasing p_0. Except in the case of $\theta_d = 30°$, the detonation wave recovered via a transverse detonation wave. The distance from the vertex of the channel corner to the point where the transverse detonation wave reflected on the lower channel wall (= wall reflection distance) was 10 - 15 times the cell width regardless of the kind of test mixture or initial pressure. We conducted numerical simulation with two-dimensional Euler equation and verified re-initiation and fan-like structure. With regard to two-dimensional detonation diffraction, whether the mixture is unstable or stable is secondary to the diffracting structure. The diffracting structure is defined roughly by only the cell width.

Acknowledgements

This work was subsidized by the Ministry of Education, Culture, Sports, Science and Technology, a Grant-in-Aid for Scientific Research (A), No. 20241040; a Grant-in-Aid for Scientific Research (B), No. 21360411; and the Research Grant Program from the Institute of Space and Astronautical Science, the Japan Aerospace Exploration Agency.

References

[1] Y.B. Zeldvich, S.M. Kogarko, N.N. Simonov, Sov. Phys. Tech. Phys. 1 (1956) 1689-1713.

[2] D.H. Edwards, G.O. Thomas, M.A. Nettleton, J. Fluid Mech. 1 (95) (1979) 79-96.

[3] R. Knystautas, J.H. Lee, C.M. Guirao, Combust. Flame 48 (1982) 63-83.

[4] S.B. Murray, J. H. Lee, Combust. Flame 52 (1983) 269-289.

[5] G.B. Whitham, J. Fluid Mech. 2 (1957) 145-171.

[6] F. Bartlma, K. Schroder, Combust. Flame 66 (1986) 237-248.

[7] B. W. Skews, J. Fluid Mech. 29 (4) (1967) 705-719.

[8] B. Khasainov, H.N. Presles, D. Desbordes, P. Demontis, P. Vidal. Shock Waves 14 (3) (2005) 187-192.

[9] N. Nagutra, J. Kasahara, A. Matsuo, Shock Waves (submitted September 12, 2011).

[10] M. Arrienti, J.E. Shepherd, J. Fluid Mech 529 (2005) 117-146.

[11] F. Pintgen, J. E. Shepherd, Combust. Flame 156 (2009) 665-677.

[12] J.H. Lee, The Detonation Phenomenon, Cambridge University Press, New York, USA, 2008, pp. 327-339.

[13] H. Nakayama, T. Moriya, J. Kasahara, A. Matsuo, I. Sasamoto, I. Funaki, Combust. Frame 159 (2012) 859-869.

[14] M. Kaneshige, J. E. Shepherd, Detonation Database**.** Technical Report FM97-8, GALCIT (1997), available at <http://www.galcit.caltech.edu/detn_db /html/>.

[15] C. W. Shu, S. Osher, J. Comput. Phys. 83 (1989) 32 - 78.

[16] V. P. Korobeinikov, V. A. Levin, V. V. Markov, G. G. Cher, Astronaut. Acta 17 (1972) 529-537.

List of Table and Figure captions

Table 1 Experimental conditions of MSOP

Gas mixture	θ_d [degree] ±0.2 °	W [mm] ±0.1 mm	p_0 [kPa] ±0.1 kPa	λ [mm] ±0.01 mm	V_{CJ} [m/s] ±1 m/s
C_2H_4+3O_2	90.0	2.0	51.1	0.83	2343
2C_2H_2+5O_2+21Ar	90.0	2.0	101.5	0.73	2378

((6 text line + 2 blanks) x 7.6 words/line x 2 column = 122 words)

Table 2 Experimental conditions of shadowgraph

Gas mixture	T [K] ±2.5 K	θ_d [degree] ±0.2°	W [mm] ±0.1 mm	p_0 [kPa] ±0.1 kPa	λ [mm] ±0.01 mm	
$C_2H_4+3O_2$	296 - 300	30.0 - 150.0	16	15.8 - 102.3	3.1 - 0.38	$\lambda = 72.31\, p_0^{-1.136}$
$2C_2H_2+5O_2+7Ar$	291 - 295	30.0 - 150.0	16	21.2 - 101.4	2.0 - 0.35	$\lambda = 61.52\, p_0^{-1.117}$
$2C_2H_2+5O_2+21Ar$	290 - 294	30.0 - 150.0	16	31.2 - 101.3	2.8 - 0.73	$\lambda = 145.3\, p_0^{-1.146}$

((7 text line + 2 blanks) x 7.6 words/line x 2 column = 137 words)

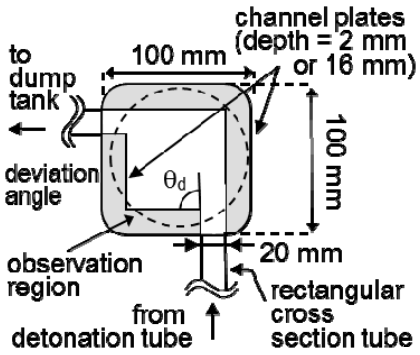

Fig. 1. Side view of the observation chamber and the observation region

(M1: (50 mm + 10 mm) x 2.2 words/mm x 1 column + 10 words = 142 words)

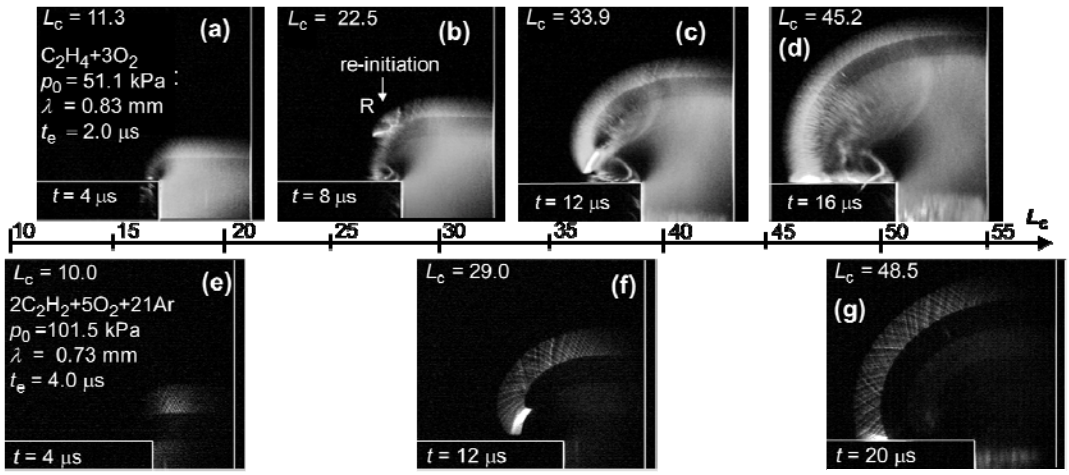

Fig. 2. MSOP image of detonation diffraction

(top is unstable mixture: C_2H_4+3O_2 and bottom is stable mixture: 2C_2H_2+5O_2+21Ar

L_c = 0 means the wave front reaches tube exit)

(M1: (62 mm + 10 mm) x 2.2 words/mm x 2 column + 26 words = 343 words)

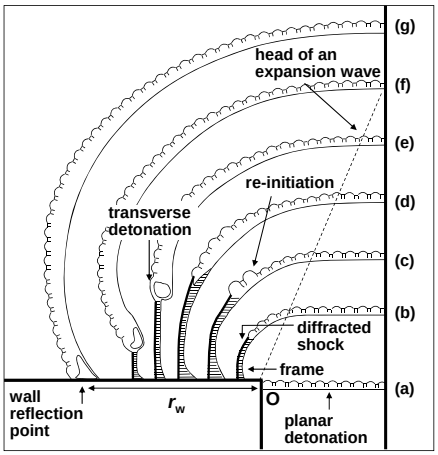

Fig. 3. Model of detonation diffraction

(M1: (60 mm + 10 mm) x 2.2 words/mm x 1 column + 4 words = 158 words)

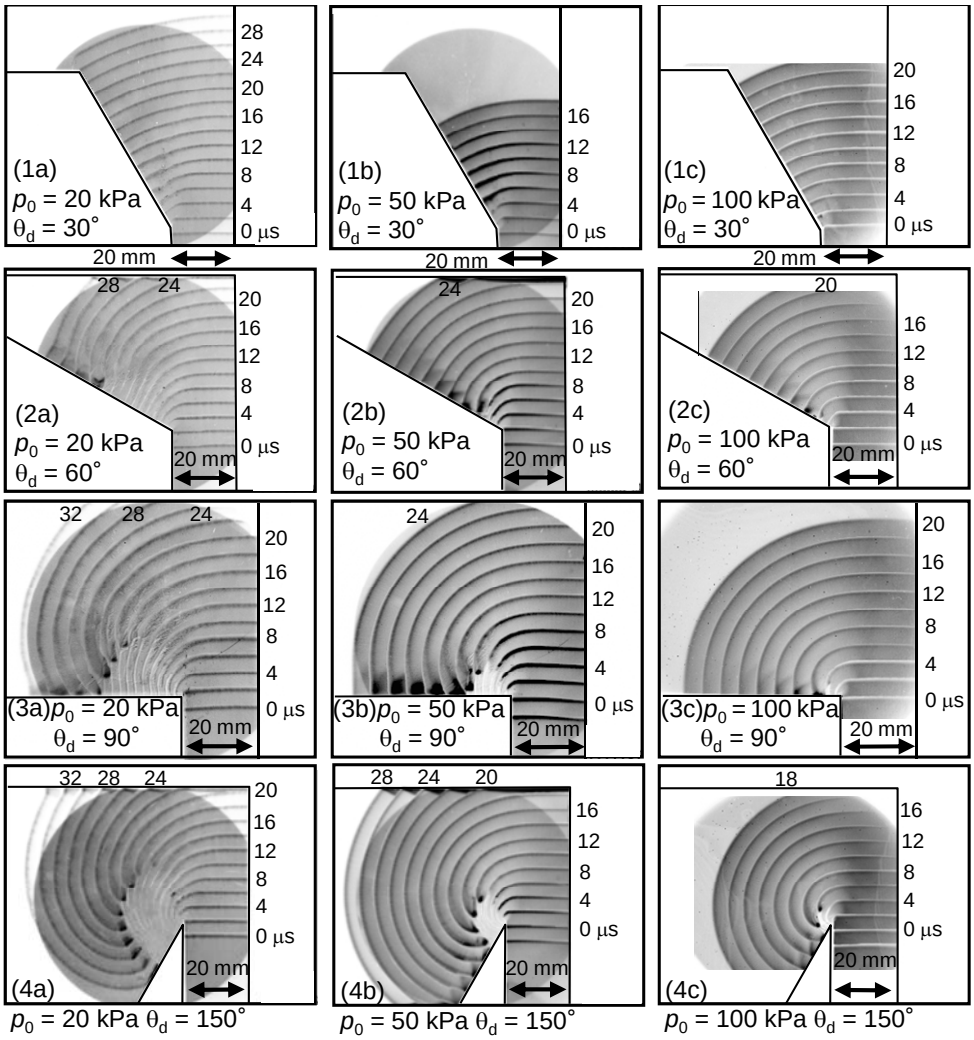

Fig. 4. Superimposed images of detonation diffraction in vertex (unstable mixture: C_2H_4+3O_2)

(M1: (139 mm + 10 mm) x 2.2 words/mm x 2 column + 10 words = 666 words)

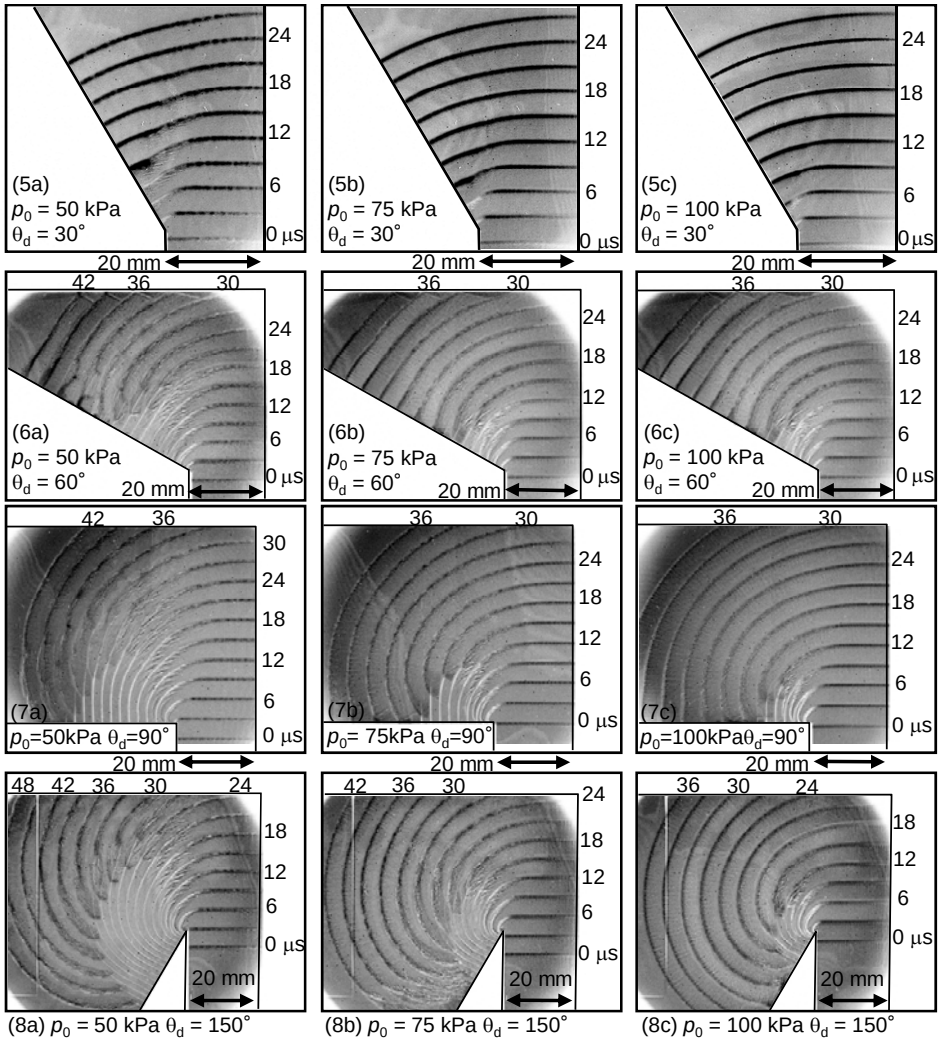

Fig. 5. Superimposed images of detonation diffraction in vertex (stable mixture: $2C_2H_2+5O_2+21Ar$)

(M1: (139 mm + 10 mm) x 2.2 words/mm x 2 column + 10 words = 666 words)

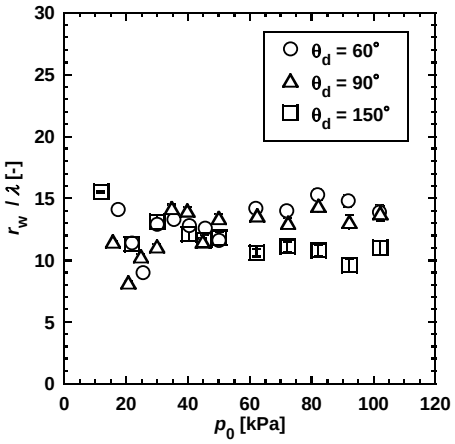

Fig. 6. Dependency of dimensionless wall reflection point on initial pressure (C_2H_4+3O_2)

(M1: (60 mm + 10 mm) x 2.2 words/mm x 1 column + 10 words = 164 words)

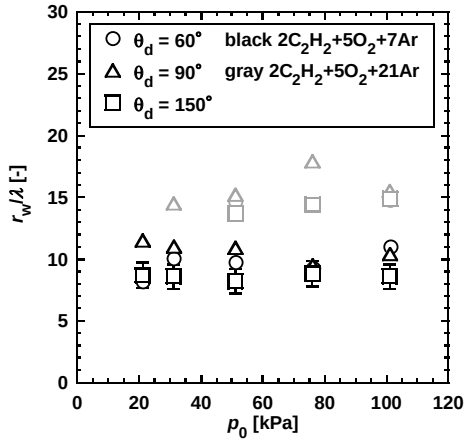

Fig. 7. Dependency of dimensionless wall reflection point on initial pressure ($2C_2H_2+5O_2+7Ar$ & $2C_2H_2+5O_2+21Ar$)

(M1: (60 mm + 10 mm) x 2.2 words/mm x 1 column + 12 words = 166 words)

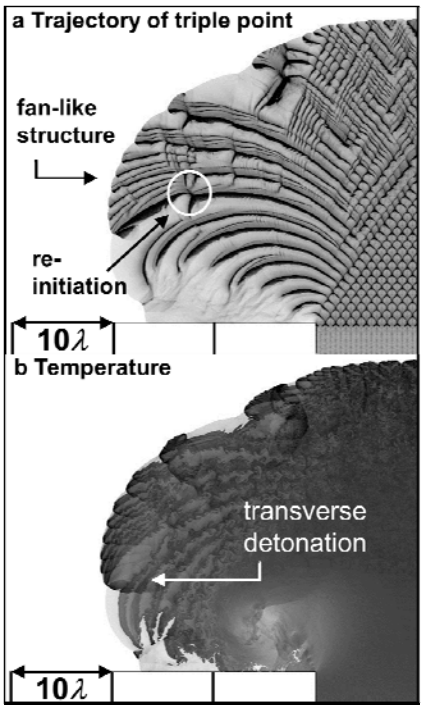

Fig. 8. Numerical simulation at deviation angle 90°
(a) Trajectory of triple point, (b) Temperature

(M1: (95 mm + 10 mm) x 2.2 words/mm x 1 column + 14 words = 245 words)